SRB THERMAL ENVIRONMENTS
FINAL REPORT

June 1989

Prepared by:

W. K. Crain
E. C. Knox
C. L. Frost
C. D. Engel

REMTECH, Inc.

Contract:

NAS8-36476

For:

National Space and Aeronautics Administration
George C. Marshall Space Flight Center
Marshall Space Flight Center, AL 35812

FOREWORD

This final report documents the SRB thermal environment work performed under the SRB REENTRY THERMAL ENVIRONMENT contract (NAS8-36476). The work was performed for the Induced Environments Branch (ED-33) for the George C. Marshall Space Flight Center (MSFC).

Contents

List of Figures

List of Tables

Section 1
INTRODUCTION

The objective of this contract was to utilize and expand the Solid Rocket Booster orbital flight test data base for better predictions of future flight environments. There were five tasks associated with this effort:

1. analyze the internal aft skirt wind tunnel data and incorporate it into a data base for generating design and preflight reentry thermal environments,
2. generate reentry design thermal environments for the SRB steel case with the nozzle extension off,
3. generate reentry design thermal environments for the SRB Filament Wound Case with the nozzle extension off,
4. develop an engineering tool to analyze the 3-D flowfield around the SRB aft skirt during reentry for the purpose of obtaining the frequency and severity of the belching gas intrusion internal to the aft skirt, and
5. perform SRM transient joint flow analysis for subscale and full scale motor firing as well as determine the effects of debonds of the insulation on the fill time and heating within the field joint insulation.

In addition, this work was extended to provide support for the 51L Shuttle SRB failure analysis.

All work items under this contract have been addressed. The purpose of this report is to document this work in summary fashion. During the course of the contract, significant results and progress were documented in monthly progress reports (RPR 142-01 through 46), and an assortment of memos, technical notes, technical reports, and design environment documents were prepared and released to the cognizant NASA offices. Details of the individual reports will not be revisited, but a summary of work performed will be presented. This work will fall under three main categories and will contain a brief description of each item, significant findings, and a list of all applicable document numbers. These categories are:

1. SRB reentry thermal environments,

2. Mission 51L SRB failure analysis support, and
3. SRM field joint redesign.

Section 2
SRB REENTRY THERMAL ENVIRONMENTS

The SRB reentry thermal environment work consists of SRB flight reentry and wind tunnel heating data analysis, incorporation of that data into a base for predicting flight environments, and design reentry environments for the Filament Wound Case and steel case both with the nozzle extension off. In addition, nozzle flame view factors were calculated to support nozzle flame environment calculations, and field joint stiffener environments at the forward and mid locations were calculated from liftoff to splashdown. Topics and reports applicable to the enclosed work are listed in Table 2.1. A brief summary of each follows.

Table 2.1: Publications Under Contract NAS8-36476

	Technical Reports
RTR 142-01	Engel, C. D., and Frost, C. L., "FWC SRB Reentry Thermal Environment," January 1986.
RTR 142-02	Engel, C. D., and Frost, C. L., "Steel Case SRB Nozzle Extension Off–Reentry Thermal Environment," January 1986.
	Technical Notes
RTN 142-01	Engel, Carl D. and Frost, Cynthia L., "FWC SRB Flight Scaled Body Point Data Base," October 1985.
RTN 142-02	Engel, Carl D. and Frost, Cynthia L., "Steel Case SRB Without Nozzle Extension Flight Scaled Body Point Data Base," November 1985.
RTN 142-03	Engel, Carl D., and Reardon, John E., "SRB Nozzle Flame View Factors," December 1985.
RTN 142-07	Engel, C. D., Bancroft, S., "Field Joint Stiffener Environments at FWD and Mid SRB Location," June 1986.
	Additional Topics
•	3D CFD Nozzle Flame/Aft Skirt Modeling
•	SRB Reentry Wind Tunnel Data Base

TOPIC: SRB Reentry Thermal Environments

These documents contain the statistical reentry design thermal environments for the filament wound and Steel Case Space Shuttle Solid Rocket Booster (SRB). Included are the necessary instructions to use the environments. The reentry environments include aerodynamic heating, aerodynamic cooling, and radiation from burning gas discharge from within the solid rocket motor (SRM). Calculated environments include nozzle flame heating and are referenced to $T_W = 600°R$. These data are intended to be used in conjunction with the ascent and separation thermal environments for the determination of the thermal protection system (TPS) requirements for reuse of the SRB when the nozzle extension is severed at apogee. These environments are based primarily on the flight data base generated from the design, development, test and evaluation (DDT&E) Shuttle flights and the operational trajectories, along with a statistical methodology.

The reentry thermal environments have been generated using the latest aerodynamics (J. Hengel, ED32-85-33), statistical trajectory set (G. Watts, ED13-27-85) and configuration (ICD-2-00001 Revision G and F IRN's). Separation of the nozzle extension is assumed to occur near apogee.

The SRB is divided into zones and each area of interest assigned a body point within the zone. Heating rate and integrated heat load were then calculated for each body point. The trajectory set considered 200 trajectories. The aerodynamic heating characteristics of this set were analyzed to predict the range of heating that will occur and the likelihood of a certain heating load being obtained. For every body point on the SRB, four thermal environments are documented, corresponding to the 0%, 50%, 95%, and 100% heating statistics based on 200 Monte Carlo trajectories.

Heating load summary tables for each of the body points are presented as well as the parachute trajectory. An example of this is shown in Fig. 2.1 and Tables 2.2 – 2.3 for zone 9. Figure 2.1 gives the body point distribution and Tables 2.2 and 2.3 present the integrated heat load summary for the steel case SRB. Documents published under this topic are summarized in Table 2.4.

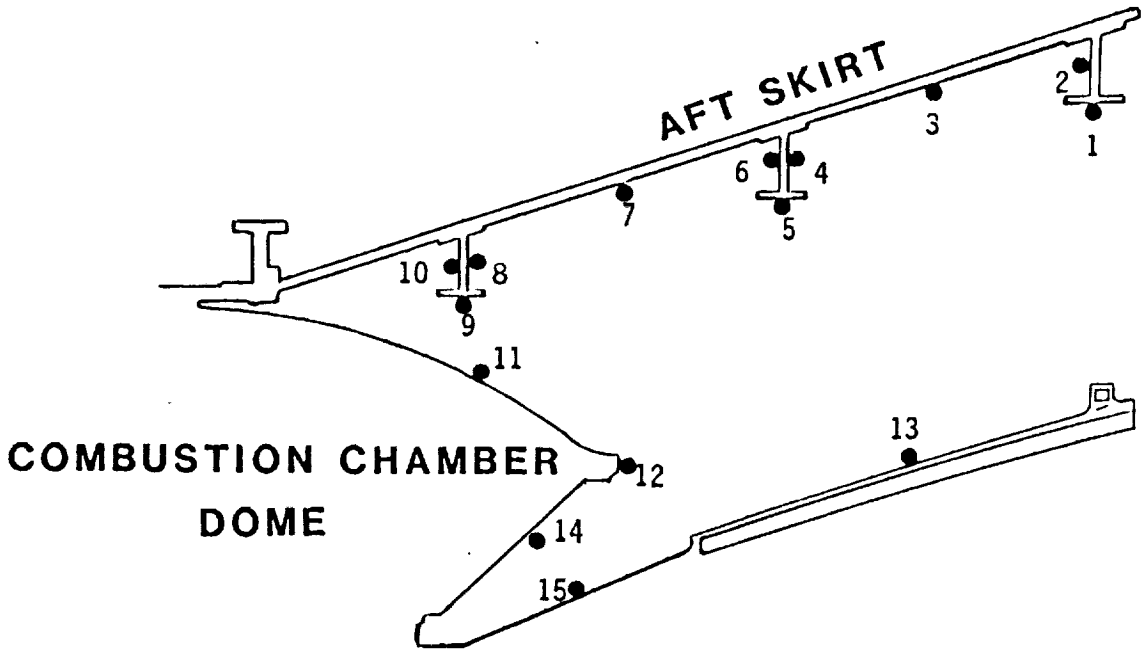

Figure 2.1: Internal Aft Skirt Body Point Distribution

Table 2.2: Statistical Thermal Environment – SC SRB Trajectory Set 1/Without Thermal Curtain/T_W = 600

				0%	50%	95%	100%
Zone 9	PT 102	Theta = .00	Load =	173.8	198.5	219.5	235.2
Zone 9	PT 103	Theta = .00	Load =	173.8	198.5	219.5	235.2
Zone 9	PT 104	Theta = .00	Load =	157.5	192.7	219.3	237.6
Zone 9	PT 106	Theta = .00	Load =	168.0	207.5	242.0	273.8
Zone 9	PT 107	Theta = .00	Load =	119.9	143.3	162.3	178.8
Zone 9	PT 108	Theta = .00	Load =	137.5	163.1	184.8	197.5
Zone 9	PT 110	Theta = .00	Load =	119.3	149.4	173.4	191.4
Zone 9	PT 111	Theta = .00	Load =	115.7	140.5	160.8	175.0
Zone 9	PT 112	Theta = .00	Load =	151.7	183.4	208.4	220.6
Zone 9	PT 113	Theta = .00	Load =	129.1	150.7	171.1	187.0
Zone 9	PT 122	Theta = 120.00	Load =	167.1	195.2	214.8	232.7
Zone 9	PT 123	Theta = 120.00	Load =	167.1	195.2	214.8	232.7
Zone 9	PT 124	Theta = 120.00	Load =	142.7	173.7	204.1	229.4
Zone 9	PT 126	Theta = 120.00	Load =	142.1	178.5	224.6	268.8
Zone 9	PT 127	Theta = 120.00	Load =	112.1	137.1	156.0	176.8
Zone 9	PT 128	Theta = 120.00	Load =	125.2	154.1	175.9	204.7
Zone 9	PT 130	Theta = 120.00	Load =	108.5	131.9	158.3	191.0
Zone 9	PT 131	Theta = 120.00	Load =	106.9	133.6	152.8	177.2
Zone 9	PT 132	Theta = 120.00	Load =	135.2	172.5	203.2	229.5
Zone 9	PT 133	Theta = 120.00	Load =	119.1	143.3	164.9	182.0
Zone 9	PT 142	Theta = 240.00	Load =	171.4	199.9	221.7	233.0
Zone 9	PT 143	Theta = 240.00	Load =	171.4	199.9	221.7	233.0
Zone 9	PT 144	Theta = 240.00	Load =	145.9	186.6	212.6	223.8
Zone 9	PT 146	Theta = 240.00	Load =	157.9	203.7	240.2	260.9
Zone 9	PT 147	Theta = 240.00	Load =	116.8	143.1	163.3	174.5
Zone 9	PT 148	Theta = 240.00	Load =	130.4	160.4	183.9	197.7
Zone 9	PT 150	Theta = 240.00	Load =	115.4	146.5	170.7	184.4
Zone 9	PT 151	Theta = 240.00	Load =	107.1	136.3	157.3	171.5
Zone 9	PT 152	Theta = 240.00	Load =	145.3	182.3	211.1	226.3
Zone 9	PT 153	Theta = 240.00	Load =	118.8	147.0	170.9	181.2

Table 2.3: Statistical Thermal Environment – SC SRB Trajectory Set 1/With Thermal Curtain/$T_W = 600$

				0%	50%	95%	100%
Zone 9	PT 102	Theta = .00	Load =	133.1	155.1	171.6	188.0
Zone 9	PT 103	Theta = .00	Load =	133.1	155.1	171.6	188.0
Zone 9	PT 104	Theta = .00	Load =	129.1	155.6	178.9	198.8
Zone 9	PT 106	Theta = .00	Load =	139.8	172.5	205.1	237.2
Zone 9	PT 107	Theta = .00	Load =	98.2	118.5	137.6	153.8
Zone 9	PT 108	Theta = .00	Load =	110.7	134.9	156.1	167.6
Zone 9	PT 110	Theta = .00	Load =	98.8	123.1	146.8	166.3
Zone 9	PT 111	Theta = .00	Load =	94.2	118.8	135.4	151.7
Zone 9	PT 112	Theta = .00	Load =	124.7	150.4	176.9	187.6
Zone 9	PT 113	Theta = .00	Load =	103.3	124.4	141.2	155.8
Zone 9	PT 122	Theta = 120.00	Load =	129.4	157.0	172.0	185.7
Zone 9	PT 123	Theta = 120.00	Load =	129.4	157.0	172.0	185.7
Zone 9	PT 124	Theta = 120.00	Load =	113.4	137.2	163.2	194.9
Zone 9	PT 126	Theta = 120.00	Load =	114.5	144.4	189.3	230.9
Zone 9	PT 127	Theta = 120.00	Load =	92.3	115.4	131.9	150.0
Zone 9	PT 128	Theta = 120.00	Load =	102.2	128.2	148.8	174.2
Zone 9	PT 130	Theta = 120.00	Load =	88.7	107.1	134.4	166.2
Zone 9	PT 131	Theta = 120.00	Load =	87.7	112.0	131.2	154.4
Zone 9	PT 132	Theta = 120.00	Load =	109.2	142.8	174.0	198.6
Zone 9	PT 133	Theta = 120.00	Load =	97.1	114.6	138.2	155.1
Zone 9	PT 142	Theta = 240.00	Load =	133.3	158.5	177.3	187.2
Zone 9	PT 143	Theta = 240.00	Load =	133.3	158.5	177.3	187.2
Zone 9	PT 144	Theta = 240.00	Load =	119.5	154.5	175.2	182.9
Zone 9	PT 146	Theta = 240.00	Load =	138.2	169.6	204.6	224.9
Zone 9	PT 147	Theta = 240.00	Load =	96.5	119.9	135.9	149.1
Zone 9	PT 148	Theta = 240.00	Load =	107.1	133.2	153.4	164.4
Zone 9	PT 150	Theta = 240.00	Load =	93.8	122.8	145.3	160.0
Zone 9	PT 151	Theta = 240.00	Load =	88.2	115.9	133.8	144.7
Zone 9	PT 152	Theta = 240.00	Load =	120.2	153.5	180.7	191.3
Zone 9	PT 153	Theta = 240.00	Load =	96.5	122.6	145.0	150.4

Table 2.4: SRB Reentry Thermal Environment Reports

DOCUMENTATION		
DOCUMENT NO.	*SUBJECT*	*DATE*
RTR 142-01	SRB Thermal Environment Data Book, Vol. II, Filament Wound Case SRB with Nozzle Extension-Off Reentry Thermal Environments	January 1986
RTR 142-02	SRB Thermal Environment Data Book, Vol. III, Steel Case SRB with Nozzle Extension-Off Reentry Thermal Environment	January 1986

TOPIC: SRB Reentry Flight Scaled Body Point Data Base

An interference factor data base for each of the gage locations on the SRB FWC and Steel Case was generated by reducing the flight heating data. The flight data was then used to replace and/or to scale the wind tunnel data. This scaling was done by the use of a multiplication factor. The scaling algorithm is defined in this report. This algorithm is defined for each of the body points. Equivalent body point numbers are given for some body points. An interference factor matrix is not generated for body points which are defined by an equivalent point.

The transformation relations (Appendix A of RTN 142-01) are read into the SRBHIHU4 code which performs the indicated function. SRBHIHU4 uses both the flight gage data base and the wind tunnel data base as input. A listing of the transformation code is given in Appendix B of RTN 142-01, and 142-02. The output from SRBHIHU4 is the flight data scaled interference factor matrix for each non-equivalenced body point. These factors were put on tape for use in generating the final environments. Reports documenting this work are listed in Table 2.5.

Table 2.5: SRB Reentry Flight Scaled Body Point Data Reports

DOCUMENTATION		
DOCUMENT NO.	*SUBJECT*	*DATE*
RTN 142-01	FWC SRB Flight Scaled Body Point Data Base	Oct. 1985
RTN 142-02	Steel Case SRB Without Nozzle Extension Flight Scaled Body Point Data Base	Nov. 1985

TOPIC: CFD Nozzle Flame/Aft Skirt Modeling

The purpose of this work was to develop a 3D CFD flowfield code to calculate the frequency and severity of the nozzle flame belching gas intrusion internal to the aft skirt. Angles of attack from 90 to 180 degrees were to be considered for both nozzle extension off and on configurations. Moreover, both supersonic, M=3.75, and subsonic, M=0.5, conditions were to be investigated. The conduct of this work was implemented through a subcontract with American Computing Inc. of Auburn, Alabama.

Work was initiated on this subcontract work on August 2, 1985, and was progressing smoothly and according to schedule through January 1986. Due to the 51L accident, this work was halted by a stop work order issued on February 14, 1986. The subcontract status at time of the stop work order is summarized in Table 2.6.

Recent advances in CFD code capabilities would make the goal of calculating nozzle flame entrainment more tractable. Thus, the technical risk of achieving the program goal is significantly reduced within the past four years. Recent flight data have shown that the nozzle flame heating can be quite significant. A renewed attempt at defining this heating mechanism is recommended for both the current SRB and the new ASRM.

Table 2.6: 3-D SRB Aft Skirt Flowfield Work

	Total Completed (%)
Task 1.1 Planning	100
Task 1.2 Basic Hydrodynamic Subroutine	
a. Coefficient Subroutines	100
b. Source Subroutines	100
c. Linear Equation Solver	100
d. Outflow Boundary Condition	75
Task 1.3 Models	
a. Scalar Coefficient Subroutines	100
b. k-equation	100
c. Epsilon Equation	100
d. Concentration Equation	100
e. Wall Functions for all six equations	90
Task 1.4 Geometry Input (Axisymmetric)	
a. Data Format	100
b. Porosity Subroutines	100
Task 1.5 Skew Differencing	
a. 2-D Polar Coordinates, Scalar	75
b. 2-D Polar Coordinates, Velocities	75
c. 3-D Cylindrical Coordinates, Scalar	50
d. 3-D Cylindrical Coordinates, Velocities	0
Task 1.6 Verification Test Cases	
a. Flow Over Cylinder	50
b. Flow Around Disk	0

Table 2.6: 3-D SRB Aft Skirt Flowfield Work (Concluded)

	Total Completed (%)
Task 1.7 Graphical Output (at Auburn)	
a. Vector Plots	50
b. Color Temperature Plots	0
Task 2.1 Input SRB Data	
a. Geometry	0
b. Exhaust Gas Properties	0
Task 2.2 Move Operation to Cray Computer	0
Task 2.3 Testing, Debugging, Solving Convergence Problems	18
Total Contract	39

The code at this point was basically written, but required debugging. A disk containing the program "as is" was delivered to MSFC on March 18, 1986.

TOPIC: SRB Nozzle Flame View Factors

In order to estimate the radiative heating external to the aft skirt due to the nozzle flame during reentry, radiative heating rates were calculated for a hypothetical flame. Relative view factors can then be determined from these radiative heating values. The heat loads for body points in Zones 8 and 9 can then be obtained by multiplying the relative view factor for a point by the reference load for that zone.

The nozzle flame was modeled as a slab with an emissive power of 100 BTU/ft-sec. The slab location and size is shown in Fig. 2.2 for the nozzle extension-on configuration. The slab was translated to $X_B = 1930.64$ for the nozzle extension-off calculations. Radiative heating rates are plotted as a function of circumferential angle from 90 to 180 degrees for 15 aft skirt regions. (An example of this is presented in Figs. 2.3 and 2.4.) The average values given on the figures are the average of all nodes shown for the component over the 90 to 180 degree interval. Each figure contains nozzle extension-on and -off data for a specific component.

View factor ratios may be obtained by ratioing the heating rates to those at another location where flight data measurements were obtained. The view factor can then be multiplied by the reference gage heating load to give the heating load at that location. To obtain the reference heating loads, the heating rates for the interval from 360.2 to 380.0 seconds were also used from 340.2 to 360.0 seconds for STS-3 and STS-5. The time, heating rate, and heating load for each of the reference gages is also presented. The report documenting this work is listed in Table 2.7.

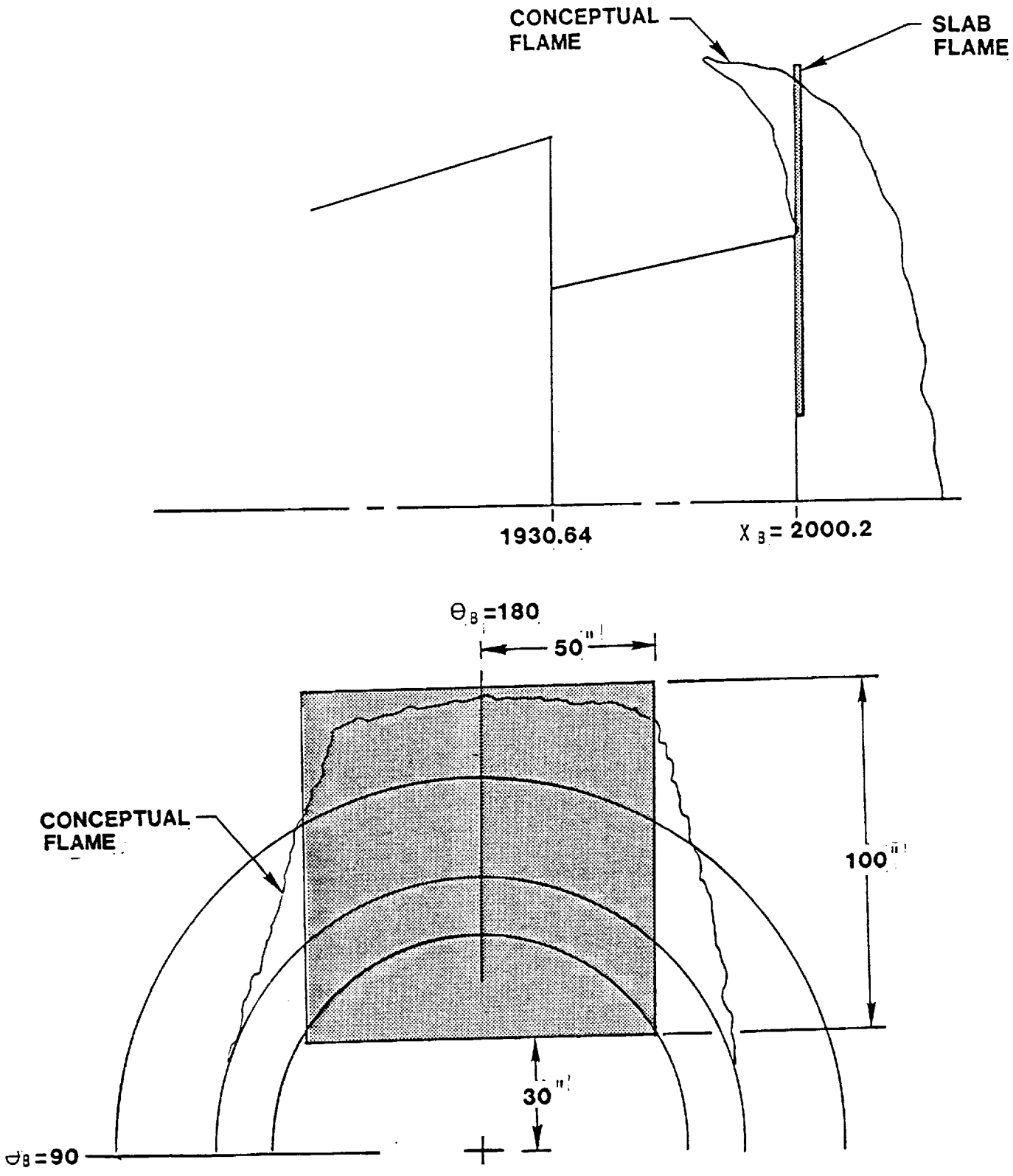

Figure 2.2: Nozzle Flame Radiation Model

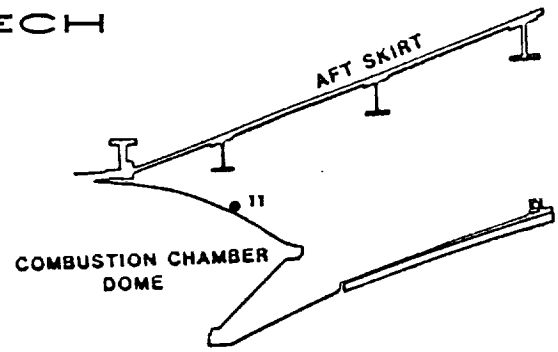

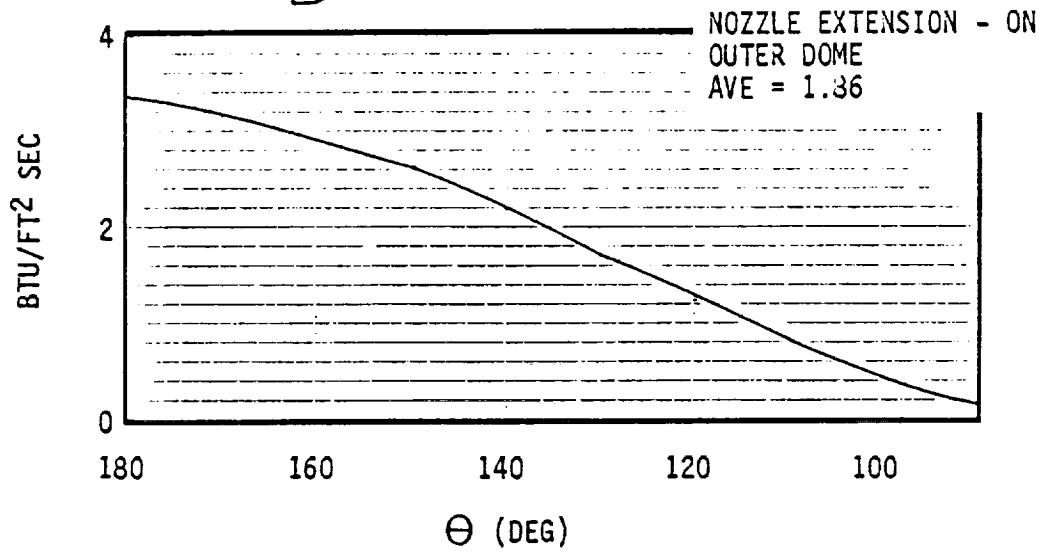

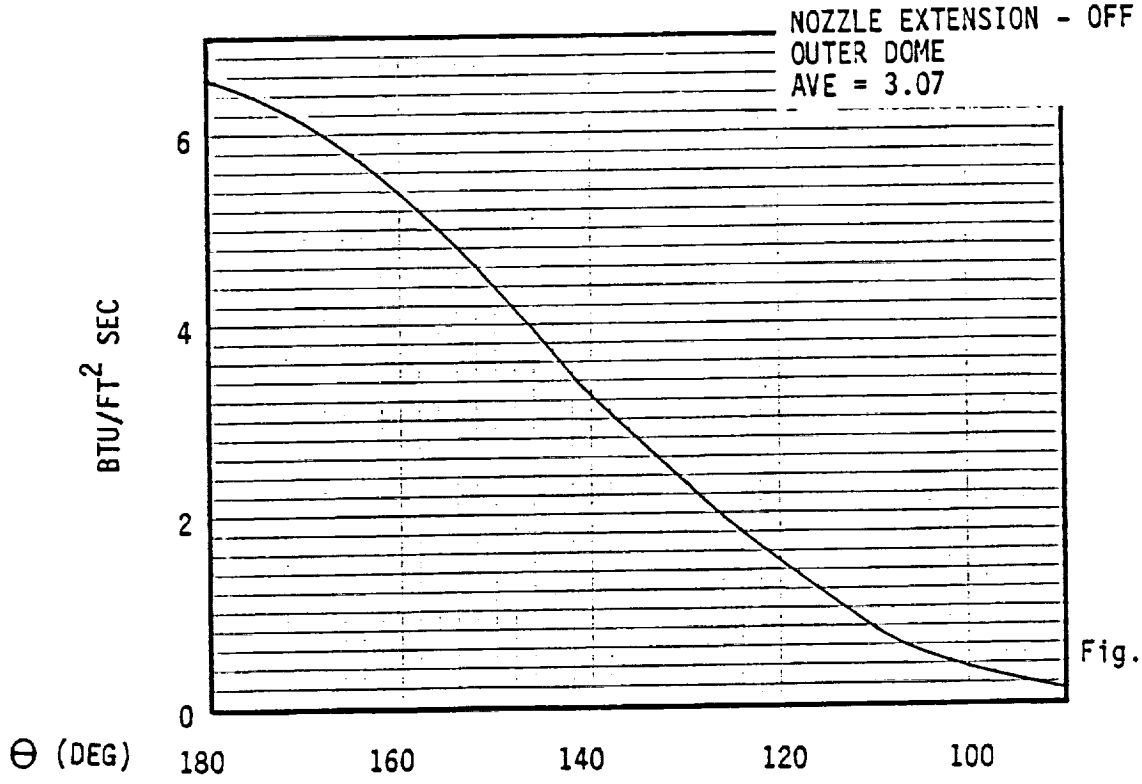

Fig. 12

Figure 2.3: Combustion Chamber Dome Heating

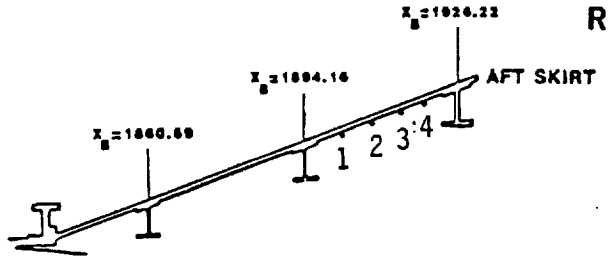

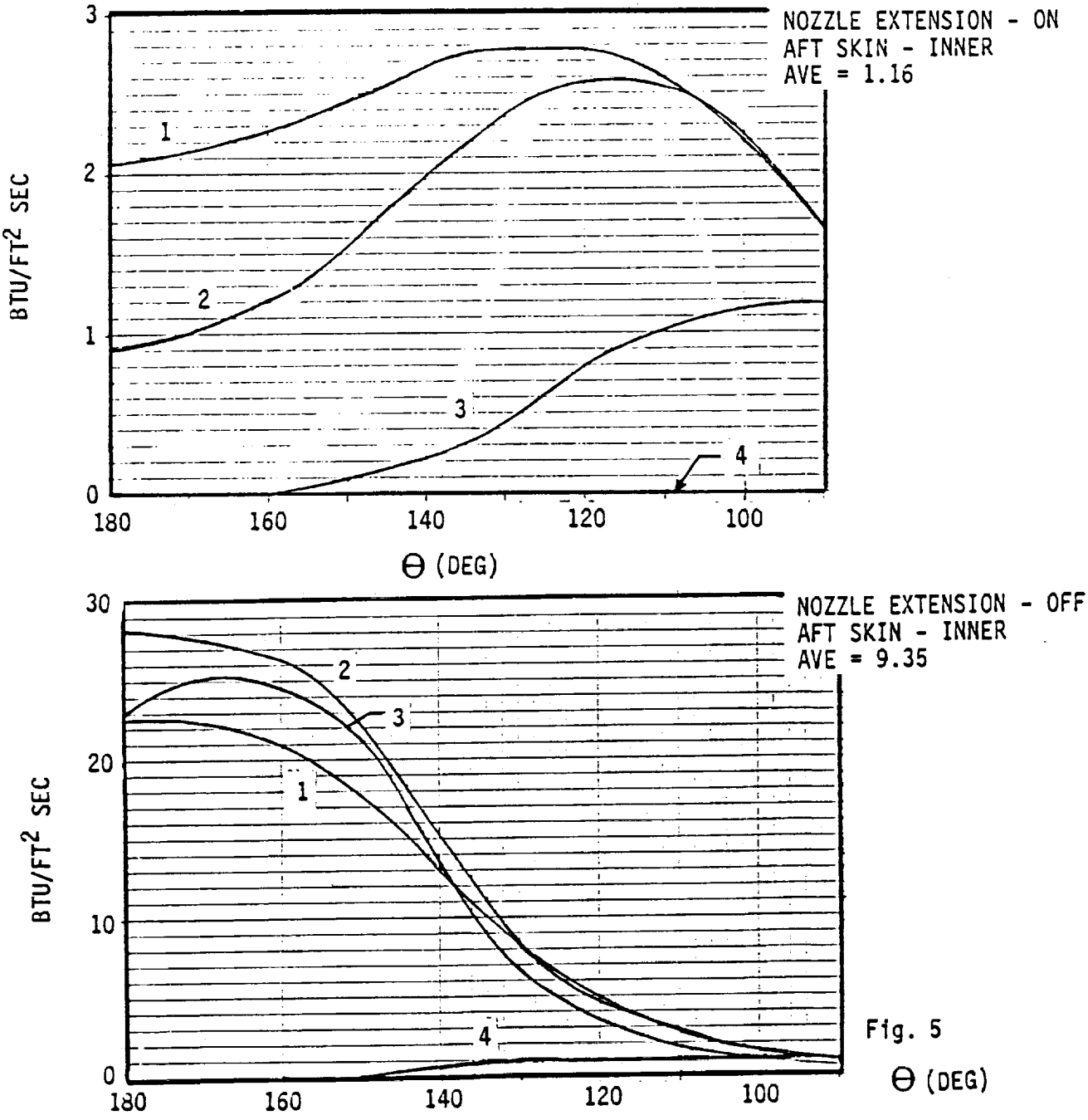

Fig. 5

Figure 2.4: Internal Aft Skirt Heating

Table 2.7: SRB Nozzle Flame View Factor Report

DOCUMENTATION		
DOCUMENT NO.	*SUBJECT*	*DATE*
RTN 142-03	Engel, Carl D., and Reardon, John E., "SRB Nozzle Flame View Factors"	Dec. 1985

TOPIC: SRB Field Joint Environments

Aerothermal environments from liftoff to splashdown for the proposed SRB field joint stiffeners (Fig. 2.5) have been developed.

The Create Environment (CREENV) computer code which has been described in RTR 094A-1 was used to generate these environments. The environments for the body points consist of three parts: ascent, plume impingement (SSME), and reentry. Ascent environment consists of plume induced convection, radiation (SRM and SSME), and ascent convection.

The different components of the environments (Code No. 12214) which were used are:

1. 1980 Ascent Environment
2. 1984 Revision "A" of 1983 SRB Operational Convective Base Heating Environment
2. 1984 Revision "A" of 1983 SRB Operational Radiation Base Heating Environment
1. 1983 Plume Impingement
4. 1984 Reentry 95 Percentile

The RDOT computer code with the recession equation for cork was used to calculate the cold wall heat loads (QCW), cold wall peak heating rates (QDCWP) and the hot wall recession rates (RHW). To get a better understanding of the various components of the environments, the heat loads and peak heating rates for the ascent aeroheating and plume convection, ascent radiation, plume impingement and aerodynamic reentry were calculated using the RDOT computer code. Heating rate versus time was plotted for the 95% Reentry ENV body points. An example of these plots is shown in Fig. 2.6. The report documenting this work is listed in Table 2.8.

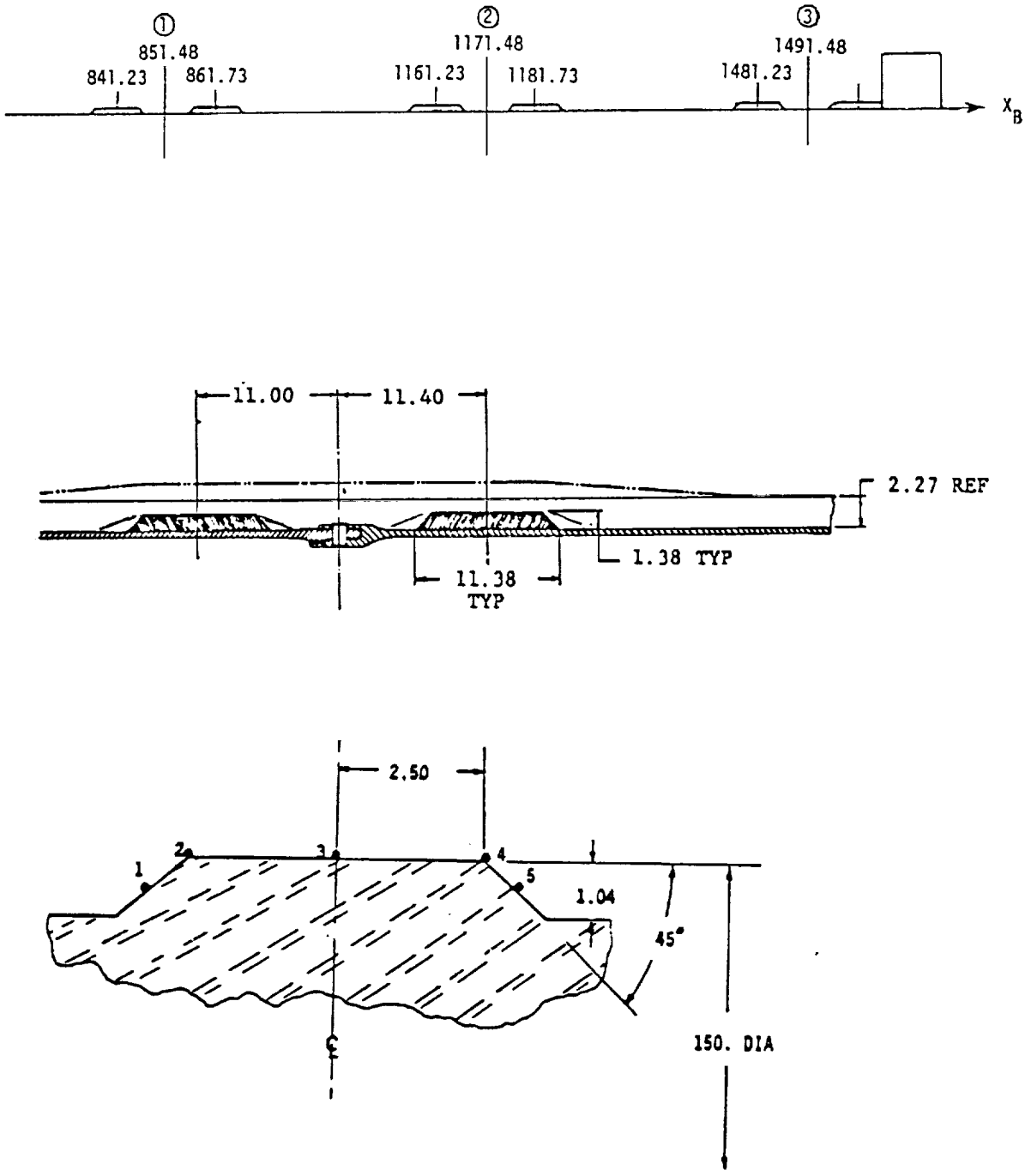

Figure 2.5: Field Joint Stiffeners

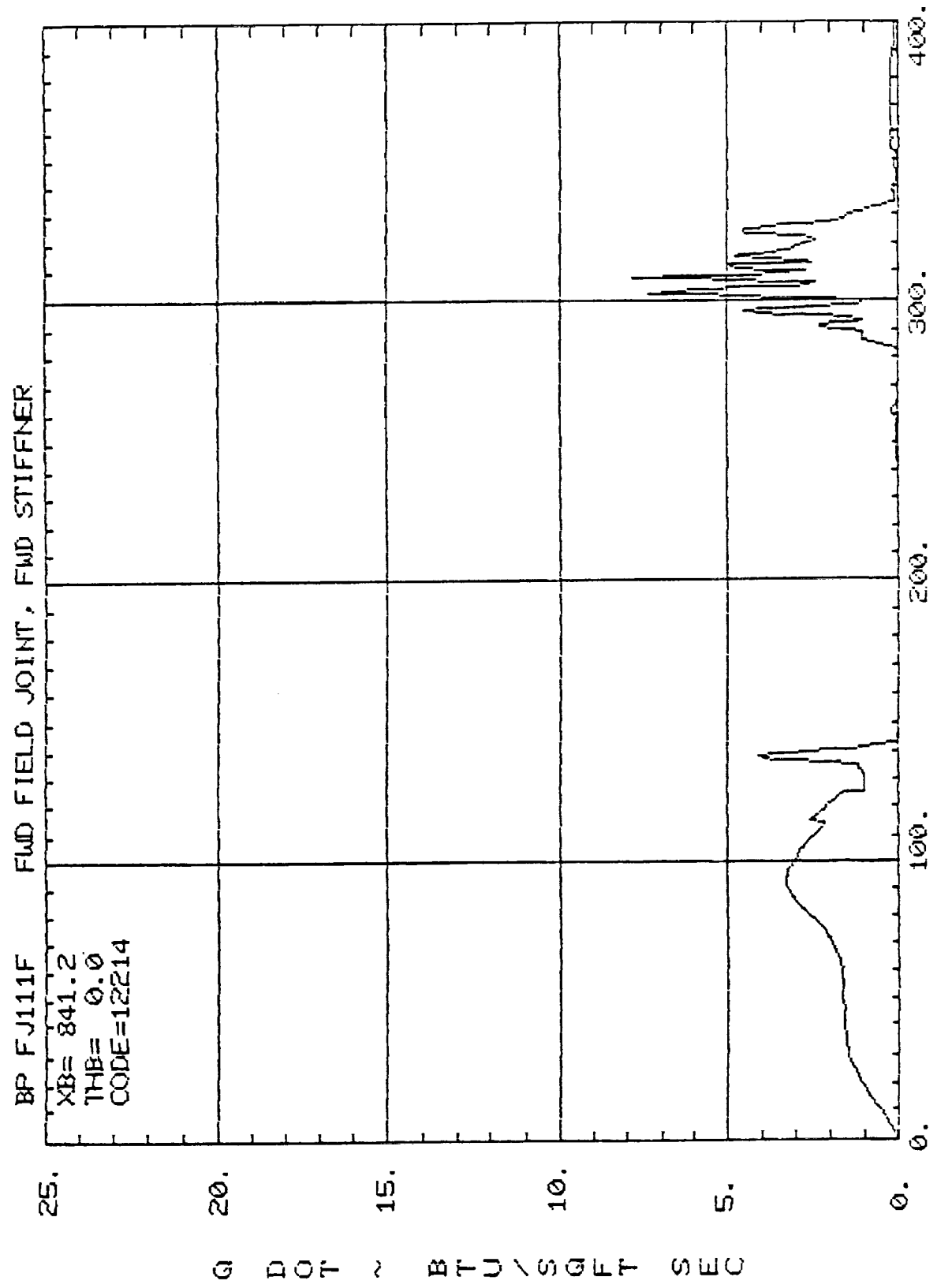

Figure 2.6: Typical Field Joint Stiffener Total Environment

Table 2.8: SRB Field Joint Environment Report

DOCUMENTATION		
DOCUMENT NO.	*SUBJECT*	*DATE*
RTN 142-07	Engel, C. D. and Bancroft, S., "Field Joint Stiffener Environments at FWD and Mid SRB Location"	June 1986

Section 3

MISSION 51L SRB FAILURE ANALYSIS

Mission 51L SRB failure analysis support work completed under this contract consists of the following:

1. Analysis of the right hand SRB field joint leak plume and comparisons with flight film,
2. Calculations of thermal environments to the right hand SRB aft separation motors,
3. Analysis of particle impingement and alumina solidification in the field joint tang/clevis gap, and
4. Upgrading of the INVENT nonadiabatic venting code used for venting analysis.

Topics and reports applicable to the enclosed work are listed in Table 3.1 with a brief description following.

Table 3.1: Topics and Applicable Reports Covered Under 51-L Failure Analysis

	Technical Notes
•	Greenwood, Terry F. and Lee, Young C., (NASA/MSFC), Bender, Robert L. and Engel, Carl D., (REMTECH, Inc.) "Shuttle Mission 51-L Right Solid Rocket Booster (R-SRB) Leak Plume Analysis," 16th JANNAF Plume Technology Meeting, Sept. 9-11, 1986.
RTN 142-04	Bender, Robert L. and Engel, Carl D., "Thermal Environments to R-SRB Aft Separation Motors During Mission 51-L," March 1986.
RTN 142-05	Bancroft, S. A., Pond, J., and Praharaj, S., "Particle Impingement Analysis, Alumina Solidification in Joint Using the EXITS Code," May 1986.
RTN 142-06	Schmitz, Craig P., "Heat Transfer Upgrades in INVENT," May 1986.

TOPIC: SRB Field Joint Leak Plume Analysis

Development of a leak plume in the R-SRB field joint forward of the attach ring was calculated along with plume geometry, flowfield and heating rates. The heating prediction contained plume convection and radiation. Impingement heating and pressure environments on the ET aft barrel section wall resulting from the SRB plume were determined and a thermal analysis of the ET run. This analysis predicted an ET burn through at approximately 64 seconds into the flight. This correlated very closely with flight film data as reported by the Presidential Commission. The methodology used in this analysis was adequate to quantify the failure conditions and validate the failure scenarios. A summary of the methodology is shown in Table 3.2. SRB leak plume impingement "footprint" on the External Tank is shown in Fig. 3.1 and the calculated impingement heating in Fig. 3.2. The report documenting this work is listed in Table 3.3.

Table 3.2: R-SRB Leak Plume Impingement on ET – Methodology Summary

OBJECTIVE	METHODS/PROCEDURES
• PLUME DEFINITION	
• Chamber Properties	CEC Code
• Throat (Hole) Conditions	CEC Code
• Plume (Inviscid)	RAMP Code
• Plume (Viscous)	BOAT Code
• Freestream Deflection	Hand Calculation
• IMPINGEMENT ENVIRONMENT	
• Heating & Pressure X/D < 75	Hand Calculation
• Heating & Pressure X/D > 75	PLIMP Code

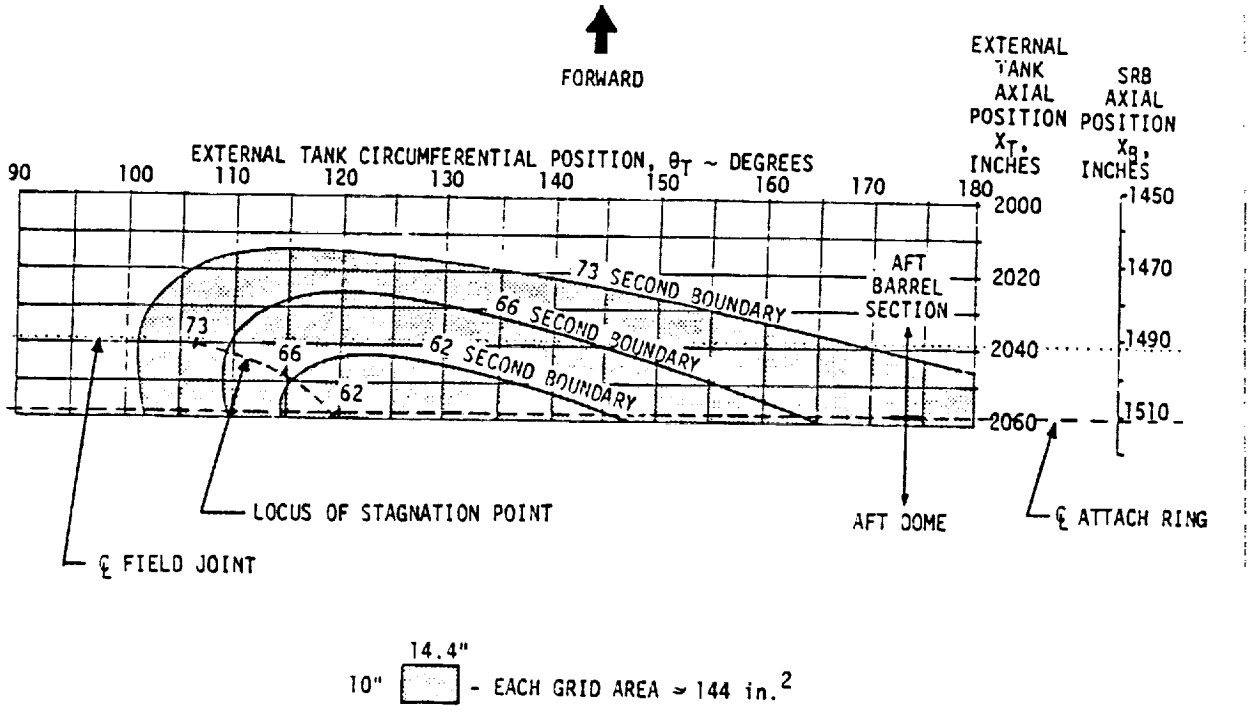

Figure 3.1: Leak Plume Impingement "Footprint" on E.T. Sidewall

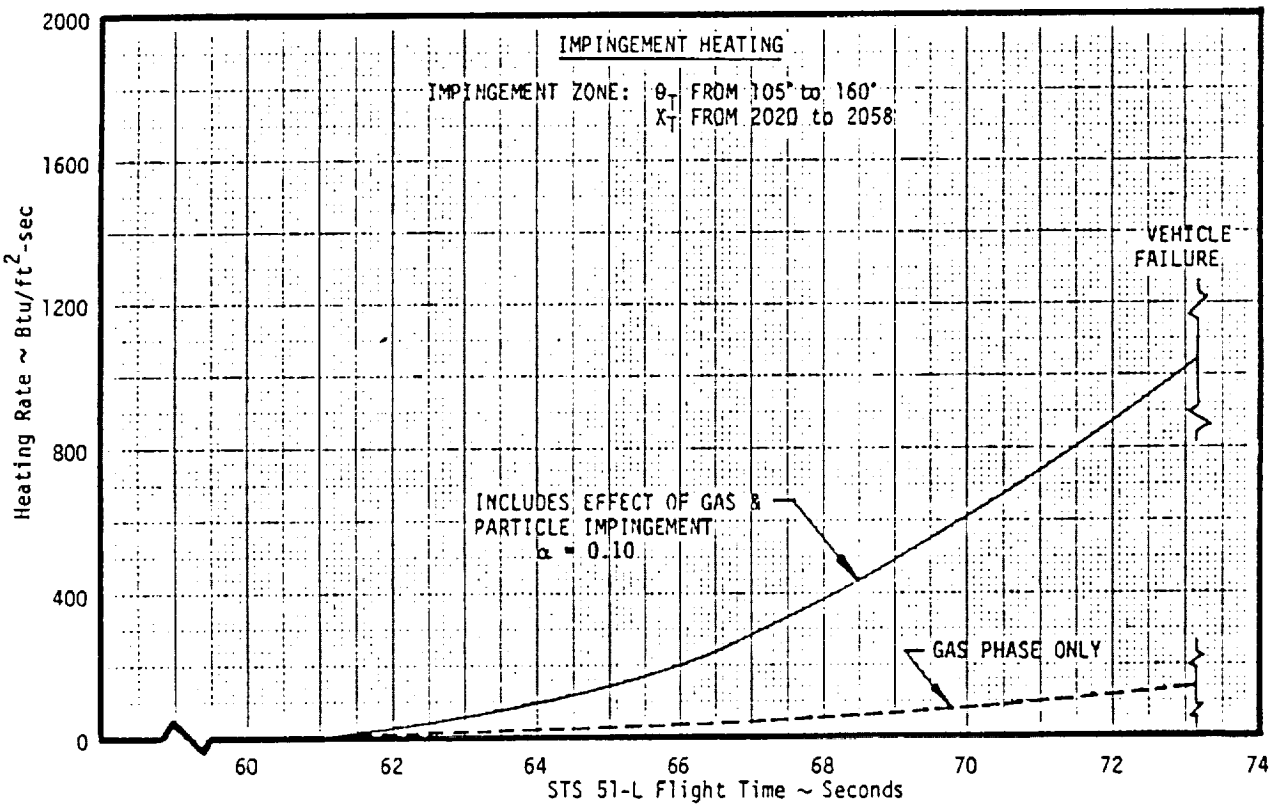

Figure 3.2: R-SRB Leak Plume Impingement Heating on E.T. Sidewall

Table 3.3: SRB Field Joint Leak Plume Analysis Report

DOCUMENTATION		
DOCUMENT NO.	*SUBJECT*	*DATE*
16th JANNAF Plume Technology Meeting, Sept. 9-11, 1986, Colorado Springs, CO	"Shuttle Mission 51-L Right Solid Rocket Booster (R-SRB) Leak Plume Analysis," Terry Greenwood and Young C. Lee (NASA/MSFC) and Robert L. Bender and Carl D. Engel (REMTECH, Inc.)	1986

TOPIC: Aft Separation Motor Thermal Environments During Mission 51-L

Environments were predicted for two locations on the inboard separation motor No. 4: design point 961 on top of the housing and design point 978 on the nozzle. These are depicted in Fig. 3.3. Estimated radiation and convective environments to these design points were calculated. The total heat load during Mission 51-L, for the design points selected, was less than that experienced during a nominal 130 second first stage boost. This work was documented in the report listed in Table 3.4.

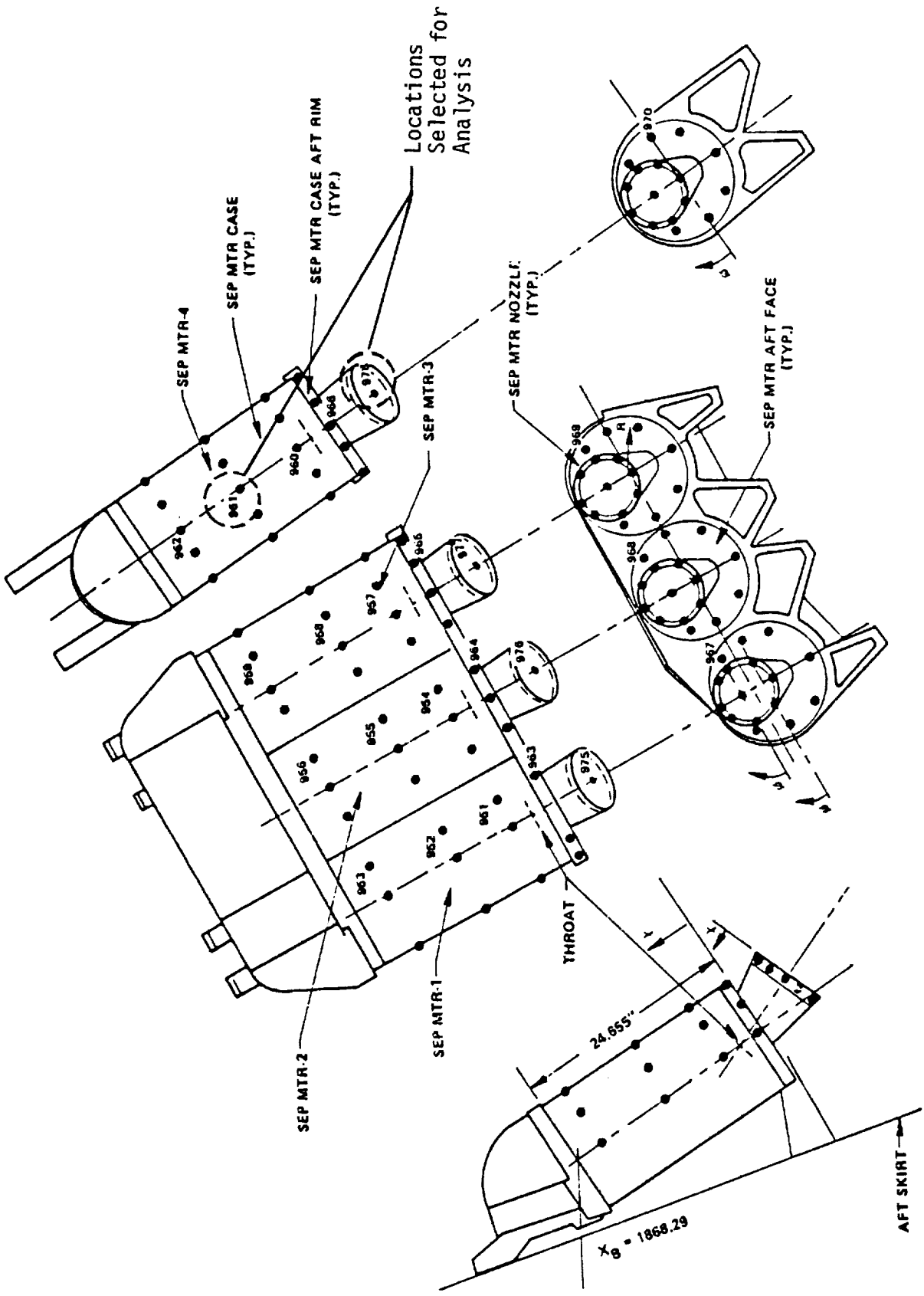

Figure 3.3: SRB Aft Separation Motor Design Point Locations

Table 3.4: Report on Aft Separation Motor Thermal Environments During Mission 51-L

DOCUMENTATION		
DOCUMENT NO.	*SUBJECT*	*DATE*
RTN 142-04	Bender, Robert L. and Engel, Carl D., "Thermal Environments to R-SRB Aft Separation Motors During Mission 51-L."	March 1986

TOPIC: Analysis of Particle Impingement and Alumina Solidification in the SRB Field Joint Tang/Clevis Gap

The EXITS computer code has been modified and updated to allow the option of particle impingement (addition of material) to the surface of the structure. The code was modified to determine the time required to deposit 0.05 in. of aluminum oxide (Al_2O_3) in the tang/clevis gap, and the amount of Al_2O_3 deposited for different area ratios. (A thickness of 0.05 in. would plug the gap.) Area ratio, mass flow and convective heat transfer calculations were made.

Conclusions of the study show that once the liquid phase is accounted for, it is improbable that a solid layer of 0.05 in. will build up by direct particle impact (Fig. 3.4). Consequently, if the gap were to be plugged by alumina solidification, a different mechanism would be required. The report documenting this work is listed in Table 3.5.

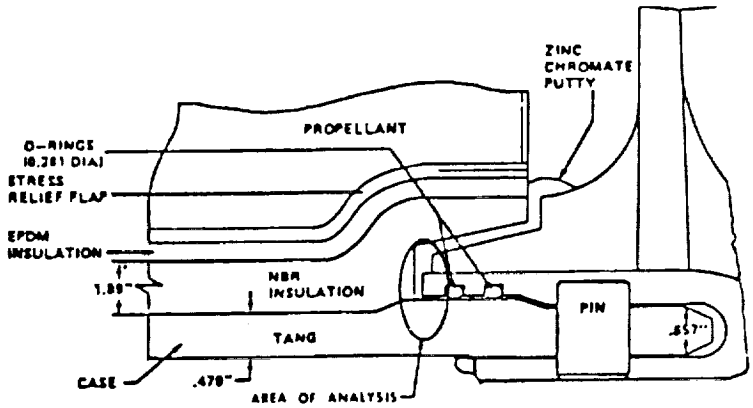

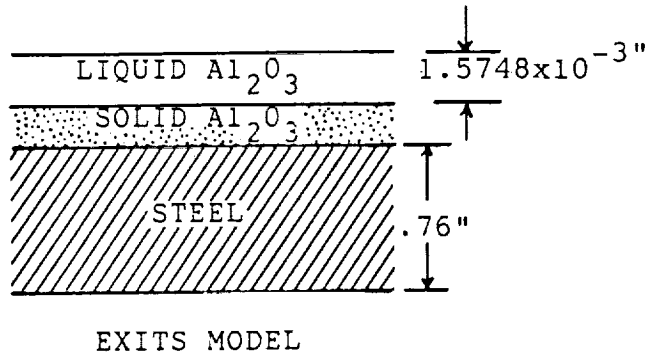

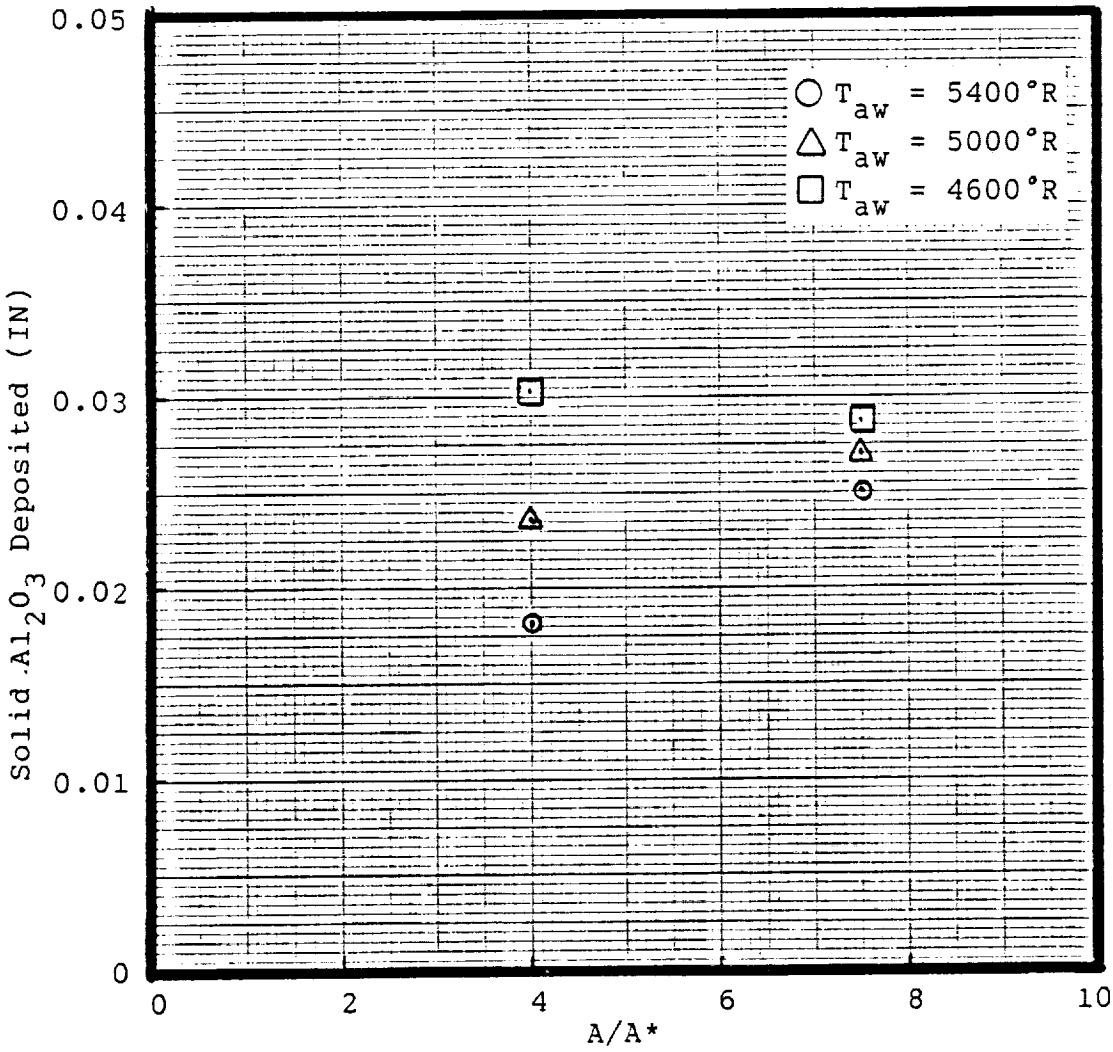

Figure 3.4: Final EXITS Result (Liquid Layer 10 Particle Diameters Thick)

Table 3.5: Report on Alumina Solidification in the SRB Field Joint Tang/Clevis Gap

DOCUMENTATION		
DOCUMENT NO.	*SUBJECT*	*DATE*
RTN 142-05	Bancroft, S., Pond, J. and Praharaj, S., "Particle Impingement Analysis, Alumina Solidification in Joint Using the EXITS Code."	May 1986

TOPIC: "INVENT" Nonadiabatic Venting Code Upgrade

The INVENT nonadiabatic venting computer code was used in support of the 51-L disaster analysis and SRB redesign effort. In an effort to verify the results created by INVENT, an analysis was performed on the heat transfer section of the code. Part of this procedure was to compare the energy balances and calculated wall temperatures generated by INVENT with similar data generated using the EXITS computer code and the analytical solution.

In several of the test cases that were performed using INVENT, the heat transfer method desired was for an infinite slab solution. In order for the user to properly model these conditions, a final temperature profile was added to the INVENT.RSL output file. The addition of outputting the temperature profile provides several important capabilities to the user of the INVENT code. One feature is that the user can ensure that semi-infinite slab conditions have been met and at the same time optimize the time requirements of the INVENT code. This is accomplished by the user selecting a "node sizing parameter" and wall thickness that results in the minimum wall thickness (with sufficient number of nodes to accurately calculate thermal gradient) that still includes a back wall node uninfluenced by the surface conditions. The report documenting this work is listed in Table 3.6.

Table 3.6: "INVENT" Nonadiabatic Venting Code Upgrade Report

DOCUMENTATION		
DOCUMENT NO.	*SUBJECT*	*DATE*
RTN 142-06	Schmitz, Craig P., "Heat Transfer Upgrades in INVENT."	May 1986

Section 4
SRM JOINT REDESIGN ANALYSIS

The fifth task under the contract was to develop computational techniques for the analysis of the flow of the hot combustion gases of the solid rocket motor into the rocket segment field and nozzle-to-case joints. Both full- and sub-scale hot motor firing test programs were initiated to examine the behavior of the hot gases as they filled the joints, some of the pre-51L design and others of candidate redesigns. The results of early subscale tests were used to refine the computational techniques and, later, the codes used to analyze selected full-scale test data and to make pretest predictions. In December 1987 end unbonds were detected between the liner and the metal case on the clevis end of motor segments delivered to KSC for use on STS-26R. The efforts to assess the effects of these unbonds on motor flight safety were supported using these analytical techniques.

All activities under this task may be categorized into topics as listed below.

1. Subscale Hot Motor Tests
2. Code Improvements
3. Pretest Predictions
4. Full-scale Motor Test Data Analysis
5. Parametric Studies
6. RSRM Field Joint Liner Unbond Analysis
7. SRB Aft Skirt Weld Failure Analysis

As stated in the Introduction, a summary discussion along with a list of published reports for each topic are presented.

TOPIC: Subscale Hot Motor Tests

The subscale tests, known as the MSFC 70-lb Motor Tests, simulated the SRM flow as illustrated in Fig. 4.1. The test field joint was of full-scale dimensions in the radial direction but the circumferential direction obviously was severely shortened. To compensate for the unsimulated circumferential volume fill bottles were attached to match the full-scale values. A total of 21 firings were made to simulate changes in the joint design as well as test the effects of flaws, or defects, in the liner seal or the O-rings allowing the hot combustion gases to fill the joint and heat up the joint materials. The defects considered were based on manufacturing tolerances and worst-case scenarios. One of the test objective was to demonstrate the fail-safe performance of the motor even with the defects.

Temperatures and pressures were measured at strategic locations in the gas flow path and a major objective in the analytical techniques was to develop confidence in the ability to predict the maximum gas temperature the O-ring would see and the amount of O-ring erosion that would occur with a given defect geometry. Shown in Fig. 4.2 is a plot of the measured and predicted gas temperature as it enters the area in front of the O-ring for a typical subscale test; Table 4.1 compares the measured and computed O-ring erosion for several of the tests.

Table 4.1: Comparison of Measured and Computed Capture-Feature O-ring Erosion for Several 70-lb Motor Tests

Test No.	Erosion, mils	
	Measured	Computed
3-3	67.	64.
3-4	129.	156.
3-5	71.	115.
3-6	90.	98.

The good agreement demonstrates achievement of that objective. The test pressures for Tests 3-4 and 3-5 indicated plugging and subsequent reopening of the flow path, which would cause the erosion to be less than computed assuming no plugging. The insights learned in the development of this capability will be discussed under the next Topic.

All the documents published under this Topic are listed in Table 4.2.

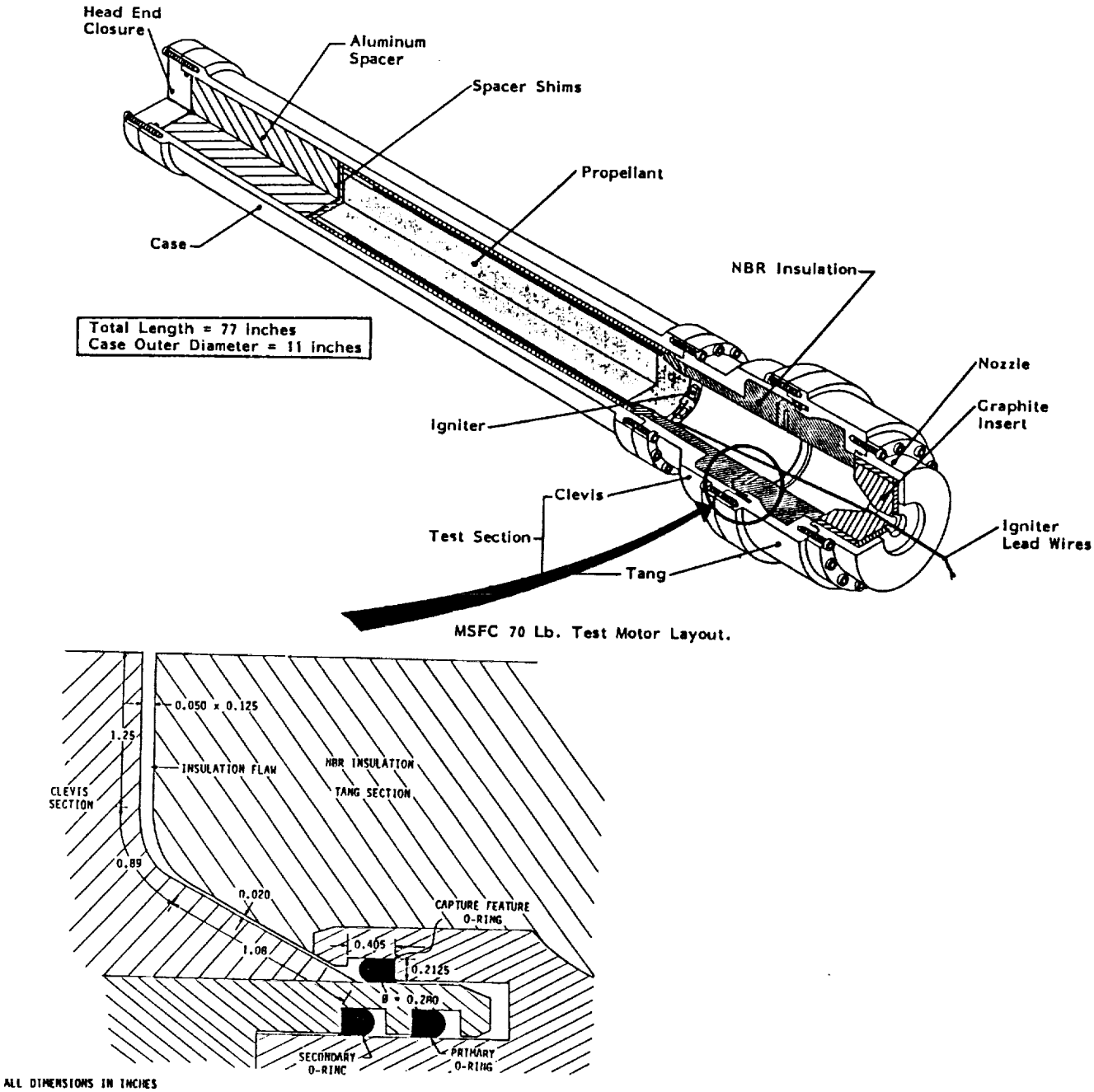

Figure 4.1: NASA/MSFC 70-lb. Motor Test Apparatus

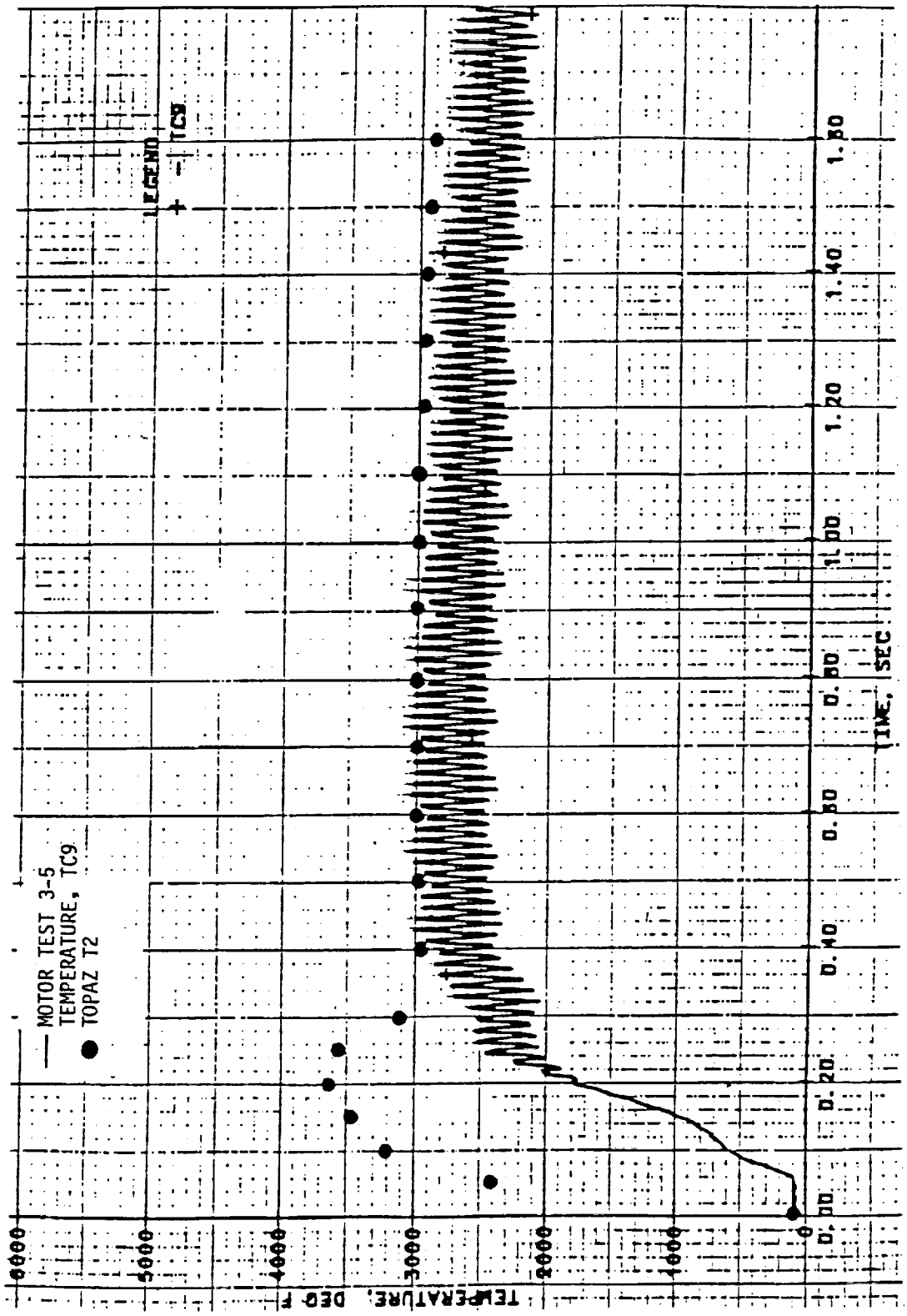

Figure 4.2: Comparison of Measured Gas Temperature Versus Time for Motor Test 3-5 with Results from TOPAZ

Table 4.2: List of Published Subscale 70-lb Motor Test Analysis Reports

DOCUMENTATION		
DOCUMENT NO.	*SUBJECT*	*DATE*
RTN 142-08	Woods, G. Hamilton and Knox, E. C., "70 Pound Motor Test 3-6 Capture O-Ring Jet Impingement Study and Erosion Prediction."	May 1987
RTN 142-08A	Knox, E. C., "70 Pound Motor Test 3-6 Capture O-Ring Jet Impingement Study and Erosion Prediction"	May 1987
RTN 142-09	Woods, G. H. and Knox, E. C., "70-Pound Motor Test 3-1 TOPAZ Flow Simulation"	May 1987
RTN 142-12	Knox, E. C., "70-Pound Motor Test 3-3 TOPAZ Simulation"	July 20, 1987
RTN 142-14	Woods, G. H., and Knox, E. C., "70-Pound Motor Test 3-2 TOPAZ Flow Simulation"	Aug. 26, 1987
RTN 142-15	Knox, E. C. and Woods, G. H., "70-Pound Motor Test 3-6 Analysis and TOPAZ Simulation Results"	Oct. 9, 1987
RTN 142-16	Nouri, Joseph A., "Analysis of 70-Pound Motor Test 3-5 and Comparison of TOPAZ Simulation and Experimental Results"	Oct. 12, 1987
RTN 142-18	Knox, E. C., "70-Pound Motor Test 3-4 TOPAZ Simulation"	Dec. 21, 1987

TOPIC: Code Improvements

The computational code used in the analytical studies was TOPAZ (Transient One-dimensional Pipe flow AnalyZer), developed at Sandia National Laboratories. The code solves the fully-coupled one-dimensional flow equations (mass, momentum, and energy) through an arbitrary arrangement of pipes, flow branches, and vessels. The code, as received, provides for mass addition (combustion), frictional losses and heat transfer to the boundaries (albeit for a constant wall temperature).

Early in the study the constraint of constant wall temperature was removed by the inclusion of an integral solution of one-dimensional heat conduction into a semi-infinite slab with a time-variant heat transfer coefficient. Also an empirical method developed by Morton Thiokol for computing the erosion of insulator-type materials such as NBR and Viton used for the motor liner and O-rings was modified to permit a change in the temperature of the gas causing the erosion and incorporated into an off-line program that uses the output from TOPAZ for the local gas pressure, velocity, and temperature in front of the O-ring to compute its erosion. The erosion model's veracity is illustrated by the comparisons given in Table 4.1, page 39.

Another innovation adopted during the study that contributed significantly to improving the modeling of the hot gas flow was the consideration that the insulation surfaces over which the hot gases flow ablates and draws some energy out of the combustion gas to fuel the ablation.

The implementation of the conduction and ablation models in the computations improved dramatically the agreement with the test results and the erosion predictions.

The documents published under this Topic are listed in Table 4.3.

Table 4.3: List of Published Code Improvements Reports

DOCUMENTATION		
DOCUMENT NO.	*SUBJECT*	*DATE*
RTN 142-11	Knox, E. C., and Woods, G. H., "Comparison of Wall Temperatures Equation in TOPAZ with the REMTECH/EXITS Code"	June 1987
RTN 142-22	Nouri, Joseph A., Knox, E. C., and Woods, G. H., "Analysis of Selected Results from NASA/MSFC (SRM D MSFC) Test 15 Using a 1-D Flow Code"	February 1988

TOPIC: Pretest Predictions

Pretest predictions for two of the 70-lb. motor tests were made, and all of the predictions indicated fail-safe operation with the built-in defects. Comparisons of the test results with the predictions were precluded because the flow path into the joint either sealed or some part of the flow path became plugged for either a part of the burn or for its duration. Similar predictions were made for the DM-8 firing but the joints sealed, preventing any gas flow from entering them.

The most comprehensive analytical predictions were done in support of the SRM Redesign Critical Design Review (Dec '87). A total of eight different joint failure scenarios were considered (four field and four nozzle/case joint geometries). An important observation from the predictions for the field joint was the significant effect of the metal/metal gap downstream of the capture feature in absorbing heat from the combustion gas passing through a failed capture-feature O-ring. The effect was sufficient to render the gas benign as it enters the volume ahead of the downstream O-rings. Also, the observation illustrated the importance of maintaining the gap dimensions in the flight hardware.

The documents published under this Topic are listed in Table 4.4.

Table 4.4: List of Published Pretest Prediction Analysis Reports

DOCUMENTATION		
DOCUMENT NO.	*SUBJECT*	*DATE*
RTN 142-10	Woods, G. H., and Knox, E. C., "70-Pound Motor Test 3-7 Capture O-Ring Jet Impingement Study and Erosion Prediction"	May 1987
RTN 142-13	Woods, G. H., and Knox, E. C., "Pretest Prediction of Erosion of Primary O-Ring Due to Jet Impingement from Defect of Nozzle/Case Joint for Full Scale Test DM-8"	Aug. 10, 1987
RTN 142-17	Knox, E. C., and Woods, G. H.,"Predictions of Gas Flow Characteristics in Simulated Flows in the Nozzle/Case and Field Joints of the Redesigned Space Shuttle SRM"	November 1987

TOPIC: Full-scale Motor Test Data Analysis

There were several full-scale motor test firings and other test articles incorporating portions of the full-scale hardware that were tested to provide additional data confirming the fail-safe operation of the redesigned joints. The full-scale motor firings and the JES and NJES test articles were tested at Wasatch and the TPTA test article as well as the 70-lb. motor tests were done at MSFC.

Of these tests data from JES 3-B was selected for analysis using the analytical techniques thus far developed. Some controversy surrounded whether or not the liner material ablated or charred as the hot gases raced through the defect in the process of filling the field joint. As discussed in a previous section, the amount of energy predicted to be available for O-ring erosion would be controlled by the selected model in the analysis. Excellent agreement with the measured gas temperature as it exited the defect was obtained using the ablation model. Shown as Fig. 4.3 is the comparison.

The one document published under this Topic is listed in Table 4.5.

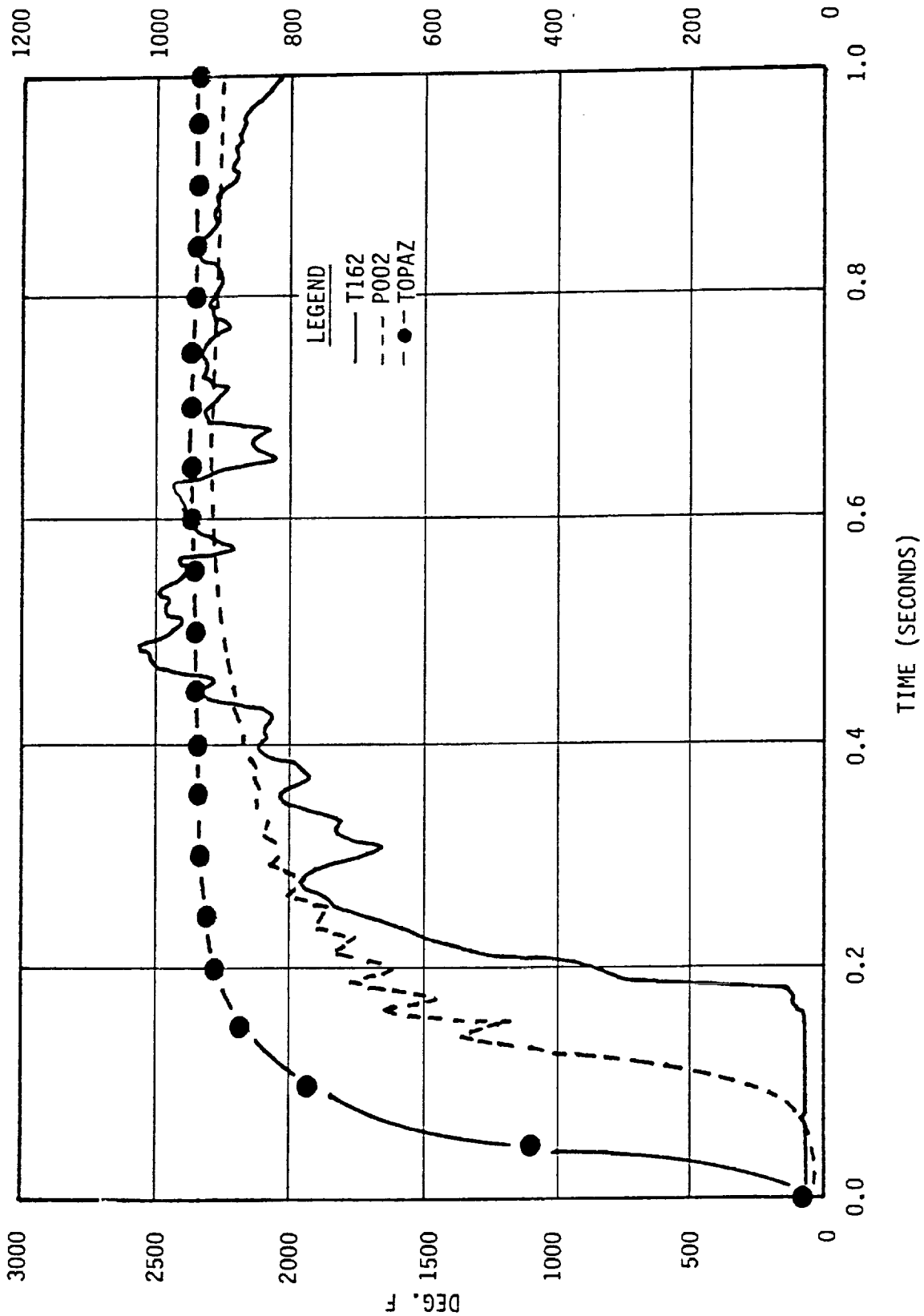

Figure 4.3: Gas Temperature History of JES-3B in Field Joint A Capture Feature in Line with Insulation Flaw (Source: 3-Hour Data Report)

Table 4.5: Full-scale Motor Test Data Analysis Reports

DOCUMENTATION		
DOCUMENT NO.	*SUBJECT*	*DATE*
RTN 142-19	Knox, E. C., and Woods, G. H., "Analysis of Preliminary Data from SRB Motor Test JES 3-B"	December 1987

TOPIC: Parametric Studies

Another objective in developing the analytical capability of computing the transient gas flow conditions in SRM joints was to perform sensitivity studies on the several parametrics that affect the gas flow. One such study was done under this Topic to examine the effect of defect size through the J-seal on the "fill time", time required for the differential from the motor bore pressure to that in the joint to become zero, and the maximum value of that differential during the filling process.

Other parametric studies were performed but they related to the unbond condition and are described under the Topic for that subject.

The one document published under this Topic is listed in Table 4.6.

Table 4.6: Parametric Studies Analysis Report

DOCUMENTATION		
DOCUMENT NO.	*SUBJECT*	*DATE*
RTN 142-20	Knox, E. C., "Parametric Study of Flow in SRM J-Seal Joints"	Dec. 31, 1987

TOPIC: RSRM Field Joint Liner Unbonds

As mentioned earlier, the RSRM segments shipped to KSC for the first post-51L shuttle flight were detected to have edge unbonds of the case liner from the steel case. Some unbonds were found on the tang side of the joint as well but the major unbonds were on the clevis side. These unbonds far exceeded the pre-51L unbond acceptance criteria. To reject them based on those criteria would cause significant launch delay, so efforts were initiated to estimate the effect of the presence of the unbonds in the joint filling process should a leak defect exist at the joint. Further, because these segments with the new joint design required a new manufacturing process, the question arose if the prior acceptance criteria were reasonable and, if not, what was.

The evolved code, TOPAZ, was used extensively in support of these efforts. The flow parameters obtained from the code were used in both 2- and 3-D conduction codes to determine steel interior temperatures around the joint with edge unbonds. These temperatures were supplied to Morton Thiokol for use in their structural stress analysis.

The pace of producing results for this effort was so rapid as to preclude the opportunity to document them until its completion. So only a report defining the techniques used to model the unbond and a summary report of the work under this Topic was published. These reports are listed in Table 4.7.

Table 4.7: List of Published RSRM Unbond Analysis Reports

DOCUMENTATION		
DOCUMENT NO.	*SUBJECT*	*DATE*
RTN 142-21	Woods, G. H., "Full Scale Modified J Seal Field Joint Insulation/Clevis Debond Model"	December 1987
RTN 142-24	Knox, E. C., and Woods, G. H., "Summary of Analysis Support for RSRM Clevis Unbonds – June/July 1988"	August 1988

TOPIC: SRB Aft Skirt Weld Failure Analysis

During the load testing of an SRB aft skirt, one of the weld seams next to a hold-down post failed over about 70 percent of its length, leaving a gap through which external gases could flow into the interior. REMTECH was asked to estimate the thermal consequences of such a scenario. The analysis and results are documented in the publication listed in Table 4.8.

Table 4.8: SRB Aft Skirt Weld Failure Analysis Report

DOCUMENTATION		
DOCUMENT NO.	*SUBJECT*	*DATE*
RTN 142-23	Woods, Hamilton, and Crain, William K., "SRB Aft Skirt Weld Seam Failure Analysis"	August 1988